carry into the monitoring of human cardiac rejection (*6*). The electrocardiogram is least discriminating during the early period after operation, especially during the first 2 weeks when nonspecific changes related to heart surgery may obscure signs of rejection. After this early period the electrocardiogram is a highly reliable indicator of rejection (*7*). The employment of LDH isozyme activities appears to meet the need for an early indicator of human cardiac allograft rejection in the first month after operation.

JAMES J. NORA
DENTON A. COOLEY
BARBARA L. JOHNSON
SHIRLEY C. WATSON
JOHN D. MILAM
Baylor University College of Medicine, Houston, Texas 77025

References and Notes

1. C. L. Markert and F. Möller, *Proc. Nat. Acad. Sci. U.S.* **45**, 753 (1959); R. D. Cahn, N. O. Kaplan, L. Levine, E. Zwilling, *Science* **136**, 962 (1962).
2. L. Cohen, J. Djordjevich, V. Ormiste, *J. Lab. Clin. Med.* **64**, 355 (1964); H. J. van der Helm, H. A. Zondag, H. A. Hartog, M. W. Van der Kooi, *Clin. Chim. Acta* **7**, 540 (1962).
3. P. G. Cabaud and F. Wroblewski, *Amer. J. Clin. Pathol.* **30**, 234 (1958).
4. J. A. Preston, R. O. Briere, J. G. Batsakis, *ibid.* **43**, 236 (1965).
5. D. A. Cooley, R. D. Bloodwell, G. L. Hallman, J. J. Nora, *J. Amer. Med. Ass.* **205**, 479 (1968); J. J. Nora, *Med Rec. Ann.* **61**, 404 (1968); D. A. Cooley, G. L. Hallman, R. D. Bloodwell, J. J. Nora, R. D. Leachman, *Amer. J. Cardiol.* **22**, 804 (1968).
6. N. E. Shumway, W. W. Angell, R. D. Wuerflein, *Transplantation* **5** (suppl. July, pt. 2), 900 (1967).
7. J. J. Nora, D. A. Cooley, D. J. Fernbach, D. G. Rochelle, J. D. Milam, J. R. Montgomery, R. D. Leachman, W. T. Butler, R. D. Rossen, R. D. Bloodwell, G. L. Hallman, J. J. Trentin, *N. Engl. J. Med.*, in press.
8. Supported by grants from the Texas Heart Institute, Houston Heart Association, and NIH grant HE-5756.

13 January 1969; revised 4 March 1969

Postsynaptic Membrane Response Predicted from Presynaptic Input Pattern in Lobster Cardiac Ganglion

Abstract. *Given the pattern of impulses impinging on a neuron, it should be possible to predict its output firing pattern if enough is known about pre- and postsynaptic properties. A quantitative reproduction of the first part of this input-output conversion is reported, namely the translation of input pattern into a sequence of postsynaptic membrane potential variations.*

A step toward the quantitative analysis of input to output conversion by the nervous system is the ability to predict the exact pattern of output impulses of a single neuron given the input pattern of presynaptic impulses converging on it. The conversion proceeds through the intermediate stage of a pattern of synaptic potentials, which is produced by the patterned presynaptic input and which in turn produces the patterned output firing. Using computer modeling techniques, we have attempted to reproduce quantitatively the first step: the conversion of a known pattern of presynaptic impulses into a pattern of postsynaptic membrane potential changes.

We used the isolated cardiac ganglion of the lobster *Homarus americanus*. This consists of nine neurons, four driver cells and five motor neurons. The drivers provide synaptic input to the motor neurons, which in turn innervate the muscle of the lobster's heart. Periodic synchronized bursts of impulses in the driver cells excite the motor cells, and the resulting bursts of motor impulses cause the heart to contract rhythmically (*1–3*). The motor neurons can be penetrated with a glass microelectrode, and the membrane potential changes associated with the burst activity can be recorded by conventional means. The impulses of individual presynaptic driver cells can be identified in simultaneous records from several pairs of extracellular electrodes (*4*). Figure 1 shows a typical intracellular record with simultaneous extracellular records on which the presynaptic impulses have been identified. Our goal was to use the times of occurrence of the identified presynaptic impulses to reproduce the observed time course of the intracellular record from the motor neuron.

The complex synaptic response of a given postsynaptic cell can be thought of as the sum of individual synaptic potentials, one for each firing of a driver cell. Each synaptic potential is characterized by (i) a delay by which its beginning follows the extracellularly observed driver cell impulse (assumed to be constant for a given driver cell); (ii) a particular shape (assumed, when scaled to fixed amplitude, to be the same for all synaptic potentials); and (iii) an amplitude, which not only is dependent on the efficacy of the synapse, but also is found to vary from impulse to impulse. The variation of amplitude is such that the closer in time the previous impulse in a given driver cell, the smaller the observed synaptic potential for the next impulse. As the interval between impulses increases, the amplitude of the synaptic potential recovers toward an asymptotic value along an approximately exponential time course with a time constant around 100 msec. This phenomenon, termed "defacilitation" or more properly "antifacilitation," also occurs in *Panulirus* cardiac ganglion (*1*).

The above-mentioned factors constitute a sufficient description of the system for the computer to generate a predicted postsynaptic response given the firing times of the presynaptic units. The critical basic parameters—delay, shape, and synaptic efficacy—were measured from intracellular records from the particular motor neuron being simulated. The uncritical antifacilitation parameters were taken to be the same for all postsynaptic units (*5*).

The firing times of the driver cells in a particular burst were then specified, and the computer calculated the individual synaptic potentials and added them together to produce the predicted membrane response for that burst (*6*). Results of this process are illustrated in Fig. 2A, which shows the predicted membrane potentials for the latter parts of three successive bursts. The corresponding actual bursts are shown in Fig. 2B. The predicted potential matches in detail the observed potential (impulses spread decrementally from axon to soma seen in bursts 2 and 3 were not simulated—see caption). The waviness of burst 1 and the smoothness of burst 2 in Fig. 2B are reproduced in the corresponding predicted bursts; in fact, almost every notch and minor peak present in the actual records is reflected in the predicted ones.

Figure 3A shows a property of certain bursts that can be explained in terms of the pattern of presynaptic impulses. The initial and final portions of the record have a wavy appearance, while the middle portion is smooth. Figure 3B shows that the phenomenon is reproduced by the computer model, while Fig. 3C shows diagrammatically the underlying pattern of presynaptic impulses responsible for it. The wavy regions correspond to the firing of all

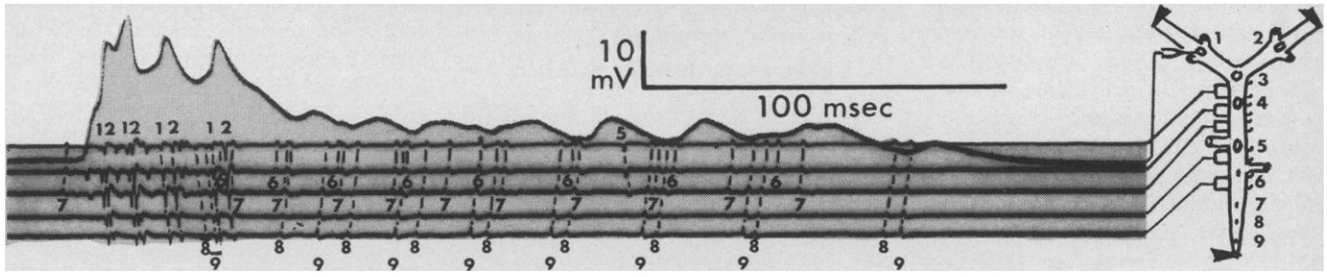

Fig. 1. Simultaneous intra- and extracellular records of a burst from the lobster cardiac ganglion. The intracellular trace is from the motor neuron designated "cell l" (see diagram at right). The five extracellular traces come from electrode pairs spaced along the median trunk of the ganglion (see diagram). Impulses from the four driver cells, "cells 6 to 9," are recorded by several of the pairs in a time-locked sequence, as indicated by lines drawn between traces. Impulse identifications, as labeled on the record, are based on which electrode pairs an impulse occurs in, impulse amplitude and shape in each pair, and the expectation of a more or less uniform discharge pattern for a given cell. Extracellular impulses from cells 1 and 2 and one from cell 5 (all motor neurons) are also labeled. Diagram: anterior up; ventral view; total length represented about 1.5 cm.

four driver cells more or less in phase, while the smooth regions correspond to the driver cells firing out of phase. All four cells are firing regular trains of impulses; but since cell 7 has a slightly higher frequency than the others, it drifts in and out of phase with them, producing synaptic potential "beats." Such phase changes among the input trains may, through their effects on the membrane potential time course, have considerable significance for the output pattern of the neuron, since postsynaptic cells fire preferentially at the higher peaks of depolarization (*1, 2, 7*).

Not all simulations were as successful as that shown in Fig. 2. In some records, impulses generated in the postsynaptic cell obscured the waveform of synaptic depolarization. In others, unexplained deviations were found. The initial part of the burst has proved difficult to simulate. Some cases where the simulation fails may lead to better insight into the properties of this ganglion. For instance, in some ganglia the average actual potential level underwent a drop where none was predicted by the model. This could be explained by the turning off of an intrinsic active response in the motor cell. The drop may be further evidence for an active response whose presence in the burst has been suggested (see *1, 8*).

We have made a few studies on the effect of altering various parameters in the model. The parameters related to rise time and peak shape of the synaptic potential and to relative synaptic efficacy seem fairly critical for a good simulation. Relative delays can only be changed by a few milliseconds, without producing a noticeably worse fit. Tentatively, the fit seems relatively insensitive to changing the antifacilitation factors.

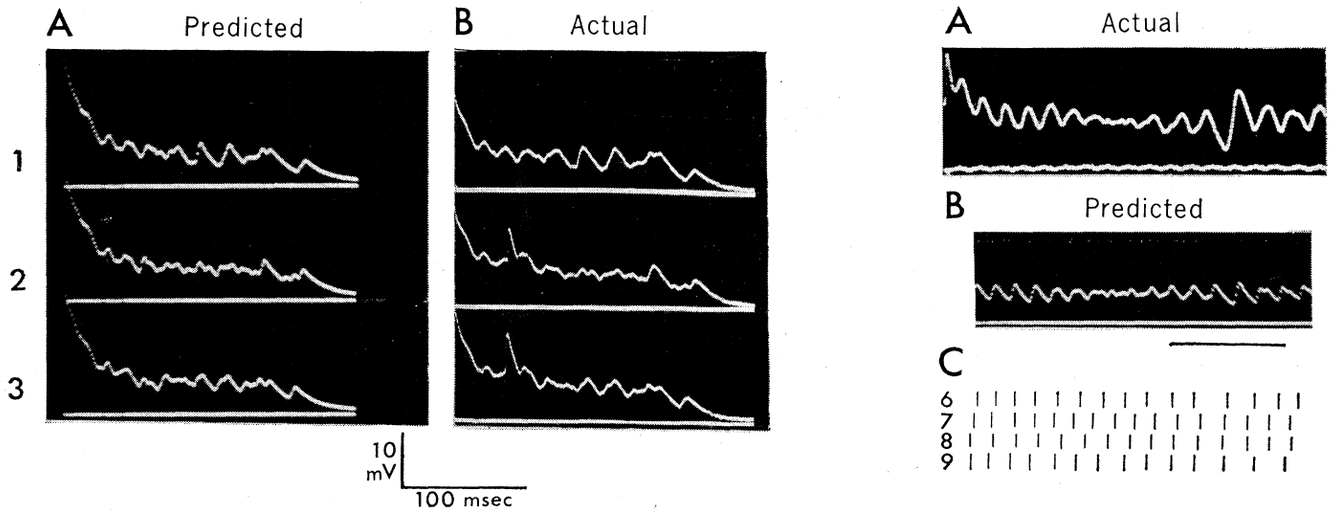

Fig. 2 (left). Comparison of predicted and actual postsynaptic responses. (A) Predicted responses for the latter parts of three successive bursts generated as described in the text from the known firing times of the presynaptic driver cells. Parameter values (*6*) were A_0's = 1.6, 1.6, 1.0, and 0.77, respectively for cells 6 to 9 (arbitrary units); d's 4, 4, 4, and 3 msec. (B) Actual responses for the same three bursts as (A). The large fast potentials near the left side in bursts 2 and 3 (not simulated by the model) are impulses fired by the motor neuron which were blocked and spread electrotonically on encountering a segment of inactive axon at a distance from the soma. Intracellular records from cell 1. Burst 1 is the same burst represented in Fig. 1. Fig. 3 (right). Synaptic potential beats. (A and B) The actual and predicted potentials, respectively, for a part of a burst in cell 2. The fast potential at the very beginning of A is an electrotonically spread impulse from the cell 2 axon. The large fluctuation near the right edge of A is not simulated well by the model for unknown reasons. Model parameters: A_0's = 0.8, 2.0, 1.1, and 0.3; d's = 7, 7, 8, and 8 msec. (C) The firing times (diagrams) of the four driver cells, cells 6 to 9, for the same portion of the burst as shown in parts (A) and (B). Wavy portions of the intracellular record correspond to driver cells firing in phase. Scale: (A) 88 msec; (B and C) 100 msec.

In summary, it is possible to model with quantitative accuracy at least some postsynaptic responses using only the times of firing of presynaptic cells and a few straightforward assumptions about their effects. It remains to go from this point to a prediction of the resulting output impulse pattern of the postsynaptic cell.

DANIEL K. HARTLINE
Department of Biological Sciences,
Stanford University,
Stanford, California 94305

IAN M. COOKE
Biological Laboratories,
Harvard University,
Cambridge, Massachusetts 02138

References and Notes

1. S. Hagiwara and T. H. Bullock, *J. Cell. Comp. Physiol.* **50**, 25 (1957); T. H. Bullock and C. A. Terzuolo, *J. Physiol.* **138**, 341 (1957).
2. D. K. Hartline, thesis, Harvard University, 1967; manuscript in preparation.
3. S. Hagiwara, *Ergeb. Biol.* **24**, 287 (1961); D. M. Maynard, in *Nervous Inhibition*, E. Florey, Ed. (Pergamon Press, New York, 1961); I. M. Cooke, *Amer. Zool.* **6**, 107 (1966); M. Anderson and I. Cooke, *Experientia*, in press.
4. D. K. Hartline, *J. Exp. Biol.* **47**, 327 (1967).
5. Delays and synaptic efficacies were measured in records from each penetration. Efficacies were obtained by measuring the amplitude of a synaptic potential from each driver cell and compensating each for its estimated antifacilitation. Time courses of synaptic potentials were measured for several ganglia and one with an appropriate shape was selected for a particular computer run. Calculated exponential tails were fitted to the synaptic potential since, in this region, errors introduced in measurement and by noise can add up significantly when many synaptic potentials are summed. Antifacilitation factors were assumed to be the same for all ganglia, since changes in them made little difference in the simulation. They were estimated from experiments where one or more driver cells were stimulated electrically by two pulses separated by a variable interval, from which synaptic potential amplitude was plotted against interval.
6. More mathematically, the theoretical synaptic potential amplitude for a given impulse was generated by multiplying a synaptic efficacy factor A_0, characteristic of each driver cell, by an antifacilitation factor $D = [r + 1 - \exp(-\Delta t/\tau)]$ where Δt is the time since the previous impulse in the same presynaptic unit, τ a time constant (a value of 100 msec was ordinarily used), and r a constant residual (usually set arbitrarily $= 0.1$). The theoretical membrane potential, $V(t)$, may then be described by:

$$V(t) = \sum_{i=1}^{4} \sum_{j=1}^{n_i} A^i{}_0 D^i{}_j \, f(t - [t^i{}_j + d^i]) \qquad (1)$$

where the jth impulse of the ith presynaptic cell occurs at time $t^i{}_j$ and is followed after a delay d^i by a synaptic potential whose waveform as a function of time θ from its beginning is given by $f(\theta)$. The function $V(t)$ was programmed on a PDP-8 computer made available by Dr. W. Simon of the Harvard Medical School under NIH grant 5-P07-FR00246-03.
7. J. P. Segundo, G. P. Moore, L. J. Stensaas, T. H. Bullock, *J. Exp. Biol.* **40**, 643 (1963).
8. A. Watanabe, *Jap. J. Physiol.* **8**, 305 (1958).
9. We thank E. S. Cosbey for generous assistance in analyzing data and revising the manuscript, A. Somers for programming assistance, C. Bennett for an early version of the program, J. Davis, D. Kennedy, P. Sokolove, D. Wilson for criticism of the manuscript. Supported by NIH grant 5-FI-GM-22,300 and NSF NB-00623 and GB-4315X.

13 February 1969

Antiserum to Lymphocytes and Procarbazine Compared as Immunosuppressants in Mice

Abstract. *As an immunosuppressant procarbazine was as potent as an antiserum to lymphocytes in mice. Both agents significantly prolonged survivals of skin allografts by 4 to 6 weeks. At the maximum tolerated dosage, procarbazine suppressed both circulating hemagglutinins to sheep erythrocytes and plaque-forming cells in the spleen. The antiserum to lymphocytes reduced the numbers of circulating hemagglutinins and plaque-forming cells by 94 percent. Procarbazine was administered to mice for 3 weeks before their exposure to antigen. Exposure for only 9 days, commencing 48 hours before injection of sheep erythrocytes, was less effective in suppressing the titers of hemagglutinins.*

Antiserum to lymphocytes (ALS) is a potent immunosuppressant agent (*1*). Chemical immunosuppressants do not approach the effectiveness of ALS and are more toxic. However, Floersheim (*2*) reported that procarbazine a methylhydrazine derivative, can prolong the survival of skin allografts across strong histocompatibility barriers and even induce tolerance in adult mice if allogeneic lymphoid cells were injected as well. The advantages of a "chemical" ALS are obvious, and we now report results of a comparative study in which procarbazine compared favorably with ALS as an immunosuppressant.

The procarbazine [*N*-isopropyl-α-(2-methylhydrazino)-*p*-toluamide] was synthesized as the hydrobromide. It was dissolved in apyrogenic sterile water and administered within an hour by intraperitoneal injection. The concentration was adjusted so that the daily dose could be given in a volume between 0.2 and 0.3 ml, depending on the weight of the mouse. It was given in maximally tolerated doses, usually beginning 21 days before immunization or grafting. The reason for this long treatment is not known (*2*). The antiserum to lymphocytes against mice was produced in white New Zealand rabbits as described (*3*). Both the ALS and the normal rabbit serum (NRS), also obtained from white New Zealand rabbits, were sterilized by filtration under positive pressure through a series of Millipore filters. Two inbred strains of mice (Jackson Laboratories, Bar Harbor, Maine) were used for the skin-grafting experiments. The recipients were mature AKR/J male mice; the donors were C3H/HeJ male mice. The method of skin grafting was that described by Bliss (*4*).

All untreated grafted control mice rejected their allografts with a mean survival time of 12.5 days. Survival of grafts in a group treated with ALS (Table 1) was prolonged to 44.7 days. The group given maximum tolerated doses of procarbazine beginning on day −21 before grafting and continued to day 7 after grafting (the average total dose was 74 mg per mouse) had a mean survival time of the skin allo-

Table 1. Effect of ALS and procarbazine on skin-graft survival. The donors were C3H/HeJ males; the recipients were AKR/J males. The ALS (10 ml/kg, intraperitoneally) was given on days −2, −1, days 0, 3, 6, 9, and 12. The procarbazine was administered intraperitoneally as follows: 300 mg/kg from day −21 to day −19; 150 mg/kg from day −17 to day −12; 100 mg/kg from day −11 to day 0; and 50 mg/kg from days 1 to 7.

Treatment	Number	Mean graft survival (days)	$P = .05$ (days)
None	32	12.5	12.1 – 12.9
ALS	18	44.7	40.6 – 48.8
Procarbazine	10	56.6	51.5 – 61.7

Table 2. Effect of ALS and procarbazine of the primary hemagglutinin (on day 13) response of mice immunized with 0.1 ml of a 30 percent suspension of sheep red blood cells (SRBC). The NRS (10 ml/kg) was administered intraperitoneally on days −2, −1, and on days 0, 3, 6, 9, and 12. The ALS (10 ml/kg) was given intraperitoneally on days −2, −1, 0, 3, 6, 9, and 12. The procarbazine (150 mg/kg) was given intraperitoneally from day −21 to day −2; reduced dosage (50 mg/kg) was given from day −1 to day +7 (five of the eight had to cease treatment on day +1).

Immunization (day 0)	Treatment	Number of mice with reciprocal hemagglutination titer:									
		0	2	4	16	32	64	128	256	512	2048
SRBC	NRS	1		1	1		1	1		2	1
SRBC	ALS	4	1	2	1	1		1			
None	None	2									
SRBC	None				1	3	2	1	1		
SRBC	Procarbazine	8									
None	None	2									